Stellar disc destruction by dynamical interactions in the Orion Trapezium star cluster

Portegies Zwart, S.F.

Monthly Notices
of the
ROYAL ASTRONOMICAL SOCIETY

MNRAS **457,** 313–319 (2016) doi:10.1093/mnras/stv2831

Stellar disc destruction by dynamical interactions in the Orion Trapezium star cluster

Simon F. Portegies Zwart★

Leiden Observatory, Leiden University, PO Box 9513, 2300 RA, Leiden, The Netherlands

Accepted 2015 November 30. Received 2015 November 28; in original form 2015 November 9

ABSTRACT

We compare the observed size distribution of circumstellar discs in the Orion Trapezium cluster with the results of *N*-body simulations in which we incorporated an heuristic prescription for the evolution of these discs. In our simulations, the sizes of stellar discs are affected by close encounters with other stars (with discs). We find that the observed distribution of disc sizes in the Orion Trapezium cluster is excellently reproduced by truncation due to dynamical encounters alone. The observed distribution appears to be a sensitive measure of the past dynamical history of the cluster, and therewith on the conditions of the cluster at birth. The best comparison between the observed disc-size distribution and the simulated distribution is realized with a cluster of $N = 2500 \pm 500$ stars with a half-mass radius of about 0.5 pc in virial equilibrium (with a virial ratio of $Q = 0.5$, or somewhat colder $Q \simeq 0.3$), and with a density structure according to a fractal dimension of $F \simeq 1.6$. Simulations with these parameters reproduce the observed distribution of circumstellar discs in about 0.2–0.5 Myr. We conclude that the distribution of disk sizes in the Orion Trapezium cluster is the result of dynamical interactions in the early evolution of the cluster.

Key words: methods: numerical – planet-star interactions – protoplanetary discs – circumstellar matter – stars: formation.

1 INTRODUCTION

The Trapezium cluster in the Orion nebula[1] (Huygens 1899, later named M 42, NGC 1976) is one of the closest 412 pc (Reid et al. 2009) young ∼0.3 Myr (85 per cent of the stars $\lesssim$1 Myr; Prosser et al. 1994, but see also Hillenbrand 1997 and Hillenbrand & Hartmann 1998) star-forming regions, composed of about 10^3 stars within a radius of ∼3 pc (de Zeeuw et al. 1999). Even though the cluster is nearby and about to emerge from its parental molecular cloud (López-Sepulcre et al. 2013), its age, the number of members and the origin of its spatial and kinematic structure remain uncertain. Being one of the closest relatively massive young stellar systems it forms a key to understand cluster formation and early evolution.

The close proximity of the Trapezium cluster allows detailed observations of circumstellar disc sizes using *Hubble Space Telescope* (*HST*)/Wide Field Planetary Camera2 (Vicente & Alves 2005). This size distribution is well characterized by a power law (Vicente & Alves 2005), but the origin of this distribution remains uncertain. Dynamical interactions in young clusters have been demonstrated to be important for the sizes of circumstellar discs in observations (de Juan Ovelar et al. 2012) as well as from a computational perspective (Vincke, Breslau & Pfalzner 2015), and the majority of protoplanetary discs are likely to be truncated by close stellar encounters (Scally & Clarke 2001; Olczak, Pfalzner & Spurzem 2006; Rosotti et al. 2014). It is however, not clear whether in the Trapezium this process can still be recognized in the observed distribution of circumstellar discs. Vicente & Alves (2005) argue that: albeit the young age of the Trapezium, and given that disc destruction is well underway, it is perhaps too late to tell if the present day disc-size distribution is primordial or if it is a consequence of the massive star formation environment.

Here, we show that the size distribution of the observed circumstellar discs is consistent with the disc-size distribution that results from close encounters in young star clusters born with complex structure. We subsequently use the observed distribution of disc sizes to reconstruct the history of the dynamical and kinematic and structure of the cluster.

2 METHODS

We use the Astronomical Multipurpose Software Environment (AMUSE; Portegies Zwart et al. 2009, 2013; Pelupessy et al. 2013) to carry out simulations. AMUSE allows us to generate initial conditions, combine a wide range of gravitational *N*-body packages and stellar

★ E-mail: spz@strw.leidenuniv.nl

[1] Huygens C. 1656

evolution modules together with other physical models, and process the data.

The application script is written in PYTHON, even though the scientific production codes are written in compiled languages. In this way, the generation of initial conditions and data processing is mostly done at the relatively slow script level, whereas the most demanding tasks are carried out with optimized code for high performance. The overhead introduced by opting for a scripting language for the data management is negligible.

Our production script starts by generating initial conditions for the young star cluster. The gravitational calculations are solved using the fourth-order HERMITE N-body code PH4 (Steve McMillan, private communication), with an time-step parameter $\eta = 0.01$ and a softening of 100 au.

During the integration of the equations of motion, we check for close approaches. When two stars happen to approach each other in a pre-determined encounter radius (initially 0.02 pc), we interrupt the N-body integrator after synchronizing the system to subsequently resolve the encounter.

2.1 The effect of encounters on disc size

The effect of the two-body encounter on the discs of both stars is solved semi-analytically. Once a two-body encounter is detected, we calculate the pericentre distance, q, by solving Kepler's equation (using the kepler-module from the STARLAB package; Portegies Zwart et al. 2001). Note that the closest approach may be well within the adopted softening radius of 100 au. The new disc radius for a star with mass m is calculated using (Breslau et al. 2014, which was calibrated for parabolic co-planar prograde encounters):

$$r'_{\rm disc} = 0.28q \left(\frac{m}{M}\right)^{0.32}. \quad (1)$$

Here, M is the mass of the other star. This equation is also applied for calculating the new disc radius of the encountering star. These new radii are adopted only if they are smaller than the pre-encounter disc radii. This procedure does not affect the dynamics of the system in the sense that the stars are not moved, although their total mass (star plus disc) is affected before the actual pericentre passage.

In order to reduce the number of disc truncations at runtime, and therewith the number of interrupts (and synchronizations) in the N-body integration, the new encounter distance for both stars is reset to half the pericentre distance. This prevents two stars from being detected at every integration time step while approaching pericentre, which would cause the disc to be affected repeatedly during a single encounter. This procedure therefore limits the number of encounters to the most destructive one at pericentre.

2.2 The effect of encounters on disc mass

The truncated discs of the encountering stars lose mass. We estimate the amount of mass lost from each disc using

$$\mathrm{d}m = m_{\rm disc} \frac{r_{\rm disc}^{1/2} - r_{\rm disc}'^{1/2}}{r_{\rm disc}^{1/2}}. \quad (2)$$

Both encountering stars may accrete some of the material lost from the other star's disc, which we calculate with

$$\mathrm{d}m_{\rm acc} = \mathrm{d}m f \frac{m}{M+m}. \quad (3)$$

Here, $f \leq 1$ is a mass transfer efficiency factor. Both equations are applied symmetrically in the two-body encounter, and as a consequence both stars lose some mass and gain some of what the other has lost.

After every 0.1 Myr, we synchronize the gravity solver, check for energy conservation, and dump a snapshot to file for later analysis. The energy of the N-body integrator is preserved better than $1/10^8$, which is sufficient to warrant a reliable result (Portegies Zwart & Boekholt 2014).

3 RESULTS

3.1 Initial conditions

Each calculation starts by generating a realization for the N-body model: stellar masses, positions, and velocities. Each star is subsequently provided with a disc of 10 per cent of the stellar mass and with an outer radius of $r_{\rm disc} = 400$ au. This corresponds to the maximal disc radius observed in the Trapezium cluster (Vicente & Alves 2005). It seems a bit small compared to protostellar disc sizes (Andrews et al. 2009, 2010), but for our calculations we only want to know if they are truncated below the maximum observed radius.

The choice of disc mass is somewhat arbitrary, but not inconsistent with observed masses of young protoplanetary discs (Williams & Cieza 2011). The mass of the initial disc is added to the stellar mass for the N-body integration. The change in disc mass due to encounters is self-consistently taken into account during the integration.

Stellar masses are selected randomly from a broken power law (Kroupa 2001) between 0.01 and 100 $\mathrm{M}_\odot$ (the mean mass of this mass function $\langle m \rangle \simeq 0.396\ \mathrm{M}_\odot$). The positions of the stars are selected from a fractal distribution (Goodwin & Whitworth 2004) with a fractal dimension of $F = 1.2$, 1.6, and $F = 2.0$, but additional simulations were performed using the Plummer (1911) distribution. The velocities of the stars ware initially scaled such that the cluster has virial ratio $Q = 0.1, 0.3, 0.5, 0.7$, and $Q = 1.0$. A value of $Q < 0.5$ results in rather cold initial conditions, $Q \equiv 0.5$ puts the cluster in virial equilibrium, and higher values are suitable for supervirial clusters. We varied the number of stars (from 1000 to 3500 in steps of 500) and the initial characteristic cluster radius (from 0.125 pc in steps of 2 to 1 pc).

We present an impression of the various initial conditions in Fig. 1, and the consequence of the dynamical evolution after 0.3 Myr in Fig. 2.

Every calculation was performed four times with a different random seed to generate the initial realization. In addition, the models that compared best to the observations have $R = 0.5$ pc, $Q = 0.3$ (and $Q = 0.5$), $F = 1.6$ were performed 12 times for each value of N, and with an output time resolution of 0.02 Myr.

3.2 Disc-size distribution

All calculations were stopped at an age of 1 Myr. During this period the gravitational dynamics of the stars is resolved numerically using Newton's law of motion. Close encounters result in the truncation of the circumstellar discs. Due to the absence of any other disc destruction mechanism all the evolution in the discs is the result of the dynamical encounters, and our simple disc-destruction prescription (see Section 2.1).

In Fig. 3, we present the size distribution of the discs from several of the simulations. To illustrate the wide range in disc distributions depending on the initial conditions of the simulations, we show one excellent comparison, and several less satisfactory cases.

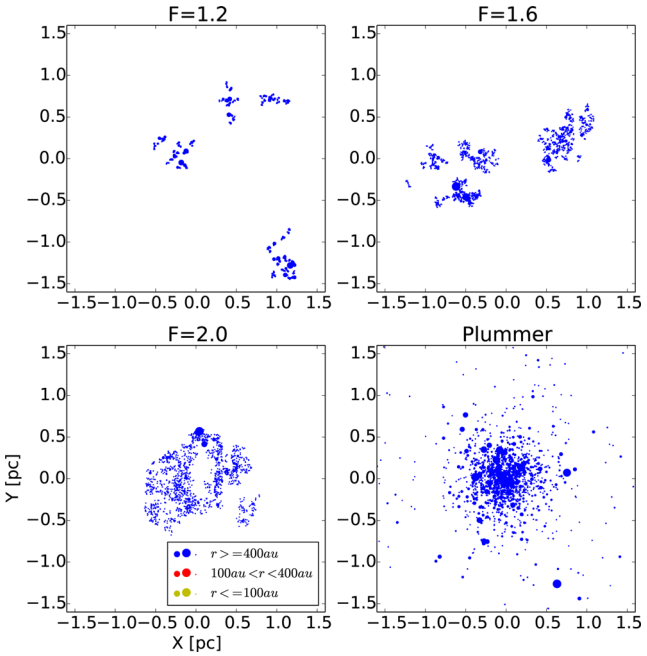

Figure 1. Initial conditions for four clusters, each composed of $N = 1500$ stars initially in virial equilibrium ($Q = 0.5$) and distributed with a characteristic radius of 0.5 pc. From the top left to the bottom right give a fractal distribution with $F = 1.2$, $F = 1.6$ (top right), $F = 2.0$ (bottom left), and a Plummer sphere (bottom right).

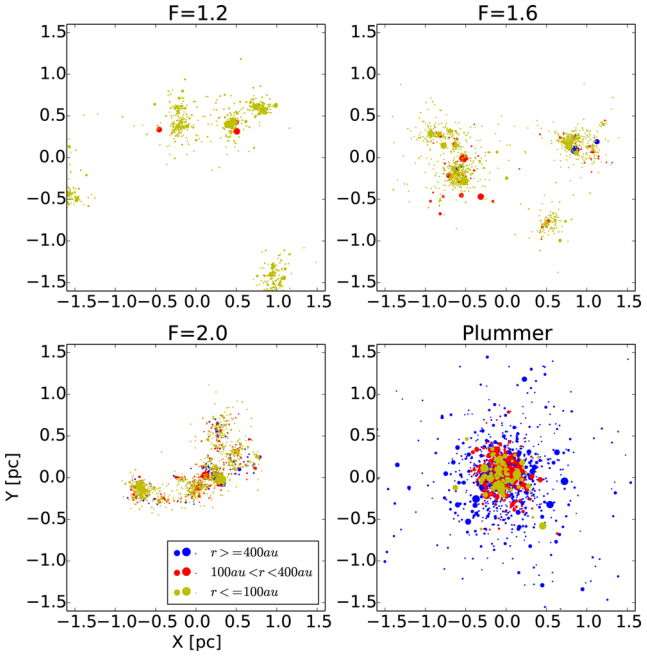

Figure 2. Presentation of four clusters from the initial conditions which we presented in Fig. 1, but evolved to 0.3 Myr. The various colours indicate the limiting radii of their discs (see bottom left for the legend).

The observed distribution is limited by the telescopes resolution (Vicente & Alves 2005). The pixel size in these observations is 45 au, and they are able to resolve discs at 1.5 pixels (or 67.5 au), although they argue that their sample is complete down to a minimum radius of 100 to 150 au. From the 162 proplyds, 95 are larger than 100 au (Vicente & Alves 2005). For the analysis, we compare

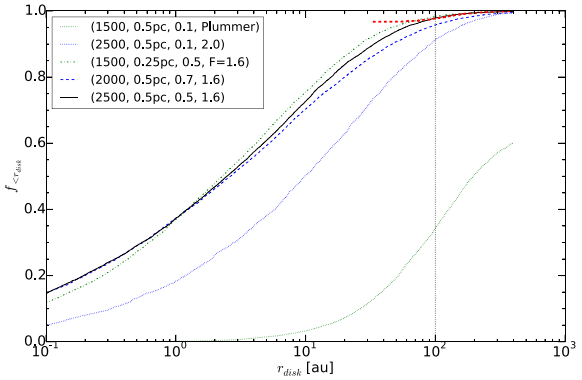

Figure 3. Cumulative radius distribution of circumstellar discs from several simulations (see top left for the legend with number of stars N, radius R in parsec, virial temperature Q, and fractal dimension F). The completeness limit in the observations at 100 au is indicated with the vertical black dotted curve. In the simulations, we are not plagued by observational election effects. The red dotted curve gives the observed disc distribution, scaled to the model with the most comparable disc distribution (solid black curve) and with the vertical offset for disc radii $\geq$100 au.

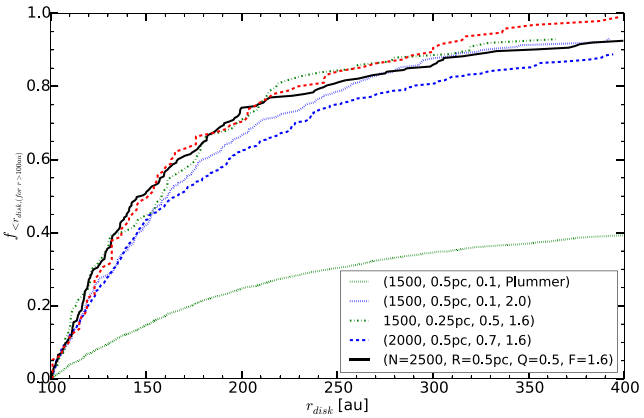

Figure 4. Cumulative size distribution of circumstellar discs in the Trapezium cluster. The observations are complete for disc radii exceeding 100 au. The red dotted curve gives the size distribution from the 95 observed discs. The other curves are the result of model simulations (with the legend indicating the simulation model parameters in the lower right corner). In contrast to the data presented in Table 1 we only show curves at an age of 0.3 Myr, whereas in the table we present the models with the highest KS-p values, which sometimes have a different age.

observed disc sizes with the simulated distribution of discs with a radius of at least 100 au.

In Fig. 4, we present the cumulative distribution of disc sizes in the simulations and compare them with the observed distribution. To better compare with the observed distribution, we only present here disc radii of 100 au and larger. The degree of consistency between the observations and simulations is expressed in the p statistics of the Kolmogorov–Smirnov (Kolmogorov 1954, KS hereafter), the Mann–Whitney–Wilcoxon (Wilcoxon 1945; Mann & Whitney 1947, hereafter MW) tests. For each of these tests, small values of the statistics p – say if $p \lesssim 0.05$ – we argue that the two distributions were sampled from different parent distributions, and these simulations are considered not to represent the observational data.

In Table 1, we present the resulting p values for the best simulations. Honestly, it is hard to make a qualitative judgment based on p values alone. We argue, however, that the number of discs with

Table 1. Results of the simulations. The top nine rows give the initial conditions for the simulations which compare best with the observations. The bottom three rows give the results of additional simulations, for which the data is also presented in the accompanying figures. The first two column gives the number of stars and the time (in Myr) at which the snapshot was compared with the observations. The following columns give the initial radius of the cluster (in parsec), the virial ratio and the fractal dimension. The subsequent three columns give the KS and NW-p values for the comparison between the observed disc distribution and the simulations, and the number of stars with a disc radius ≥100 au, which corresponds to the observational limit. The last two columns give the KS-p value for the comparison between the observed and simulated disc mass, and the number of discs in the simulations which comply to the observed limits ($m > 4.2\,M_{\rm Jupiter}$, 20 au $< r <$ 200 au, see Section 3.3).

N	t (Myr)	R (pc)	Q	F	$p_{\rm r,\,KS}$	$p_{\rm r,\,NW}$	$N_{r\,\geq\,100{\rm au}}$	$p_{\rm m,\,KS}$	$N_{20\,<\,r\,<\,200{\rm au}}$
2000	0.1	0.25	0.1	2.0	0.80	0.40	86 ± 19	0.30	236 ± 17
2500	0.1	0.25	0.1	2.0	0.84	0.39	93 ± 37	0.32	315 ± 52
2500	0.2	0.5	0.1	1.6	0.77	0.43	80 ± 24	0.50	145 ± 5
1500	0.3	0.5	0.3	1.6	0.72	0.22	78 ± 23	0.48	156 ± 30
2500	0.4	0.5	0.3	1.6	0.68	0.34	74 ± 27	0.58	193 ± 14
3000	0.3	0.5	0.3	1.6	0.70	0.50	67 ± 6	0.77	213 ± 10
2000	0.6	0.5	0.5	1.6	0.82	0.25	63 ± 9	0.76	155 ± 15
3000	0.2	0.5	0.5	1.6	0.54	0.46	80 ± 25	0.63	223 ± 30
1500	1.0	0.5	1.0	1.6	0.50	0.29	72 ± 25	0.46	144 ± 11
2000	0.2	0.5	0.7	1.6	0.02	0.01	95 ± 29	0.30	169 ± 28
1500	0.3	0.25	0.5	1.6	0.86	0.47	25 ± 10	0.66	90 ± 14
1500	0.3	0.5	0.1	Pl	0.00	0.00	986 ± 23	0.05	353 ± 17

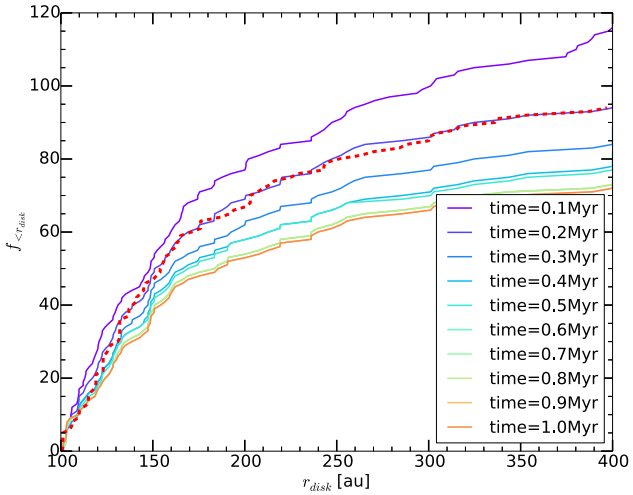

Figure 5. Time evolution of the cumulative disc-size distribution for one of our simulations with $N = 2000$ stars with $R = 0.5$ pc, $Q = 0.7$, and $F = 1.6$. This run was not included in Table 1, because even though this particular run gave a very satisfactory comparison with the observations, the other three runs did not as well and the overall value for $p = 0.024$ at $t = 0.2$ Myr. The distributions are not normalized, to show how the number of disc sizes in the observed range decreases with time. The normalized version at $t = 0.3$ Myr is also presented as the blue dashed curves in Fig. 3 (for the complete distribution) and in Fig. 4 for the normalized cumulative distribution.

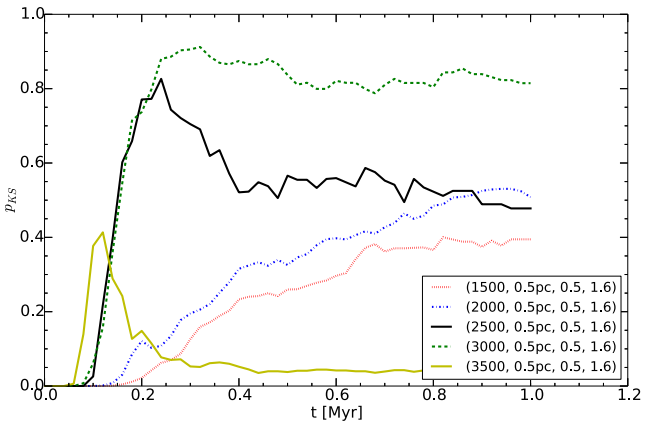

Figure 6. KS-p value for simulation with $N = 1500$ to $N = 3500$ stars with $R = 0.5$ pc, $Q = 0.5$, and fractal dimension $F = 1.6$ up to an age of 1 Myr. The KS values are calculated by summing over 12 runs for each set of parameters with a time resolution of 0.02 Myr.

a radius ≥100 au also have to be taken into account. Following Poisson statistics, we argue that the observed number of discs with a radius ≥100 au must be between 70 and 120 (if we do not take the statistics of the simulation into account). Several of our simulations resulted in satisfactory KS and MW statistics, but with so few (or so many) stars within the appropriate range that we could exclude them from further consideration. The remaining cases are listed in Table 1 (plus three ill comparisons for completeness, because those are presented also in Figs 3 and 4).

We demonstrate the evolution of the number of stars with discs $r_{\rm disc} \geq 100$ au in Fig. 5, where we present the time evolution of the distribution of disc sizes for one of the simulation. At an age of $t = 0.2$ Myr, the disc-size distribution compares well with the observed distribution, in shape as well as in number. At later age the number of stars with discs in the appropriate regime drops quite dramatically.

In Fig. 6, we present the time evolution of several simulations with a characteristic radius of $R = 0.5$ pc, a virial temperature of $Q = 0.5$, and fractal dimension $F = 1.6$. Those simulations generally result in the highest p values for KS statistics (and equivalently so for MW statistic) in comparison with the observed circumstellar disc-size distribution.

The runs with $N = 1000$ and 2000 show a steady but relatively slow rise to a KS probability $p \simeq 0.5$ on a time-scale of about 1 Myr, and the high $N = 3500$ simulation peaks at $t \simeq 0.1$ Myr but hardly exceeds $p = 0.4$. The simulations with intermediate N (between 2500 and $N = 3000$) show a promising trend of peaking around $t = 0.2$–0.3 with a maximum $p \sim 0.9$.

3.3 Disc-mass distribution

Disc masses have been determined in the Orion Trapezium cluster using millimetre observations (Mann & Williams 2009). This has

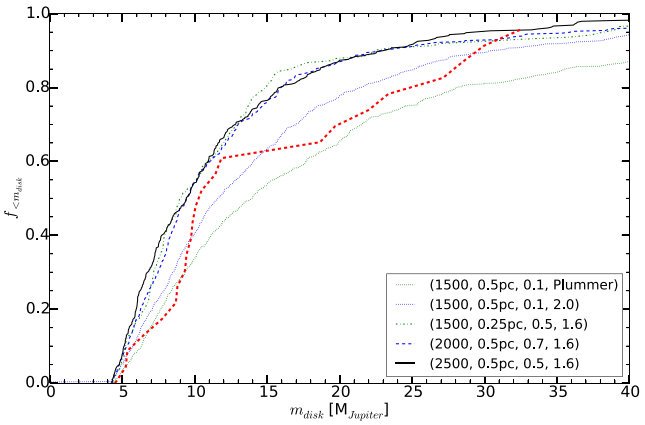

Figure 7. Cumulative distribution of disc masses in the Trapezium cluster (using $f = 1$ in equation 3). The observations are claimed to be complete down to a mass of 4.2 $M_{\rm Jupiter}$, below which we do not plot any data. There are only 23 observed discs with at least this mass. The other curves give the result of the model simulations at an age of 0.3 Myr; the legend (bottom right) explains the initial model parameters, but they are the same as in Figs 3 and 4. Except the two dotted curves (green and blue), each of these models produce a satisfactory fit to the observed disc masses. Due to the limited statistics, the disc-mass distribution generally compares much better to the observations than the disc-size distribution.

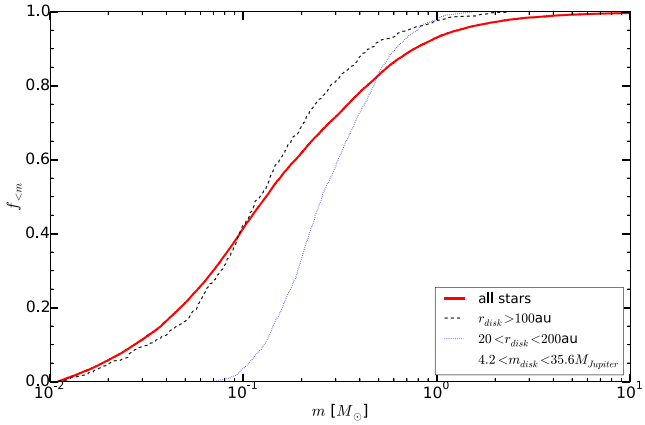

Figure 8. Cumulative distribution of stellar masses in simulation with $N = 2000$ stars, $R = 0.5$ pc, $Q = 0.5$ pc, and $F = 1.6$ at an age of 0.3 Myr. The red solid curve gives the mass function for all stars, and is identical to the initial mass function adopted for all our simulations. The black dashed curve give the mass function for the stars with a disc $r_{\rm disc} > 100$ au, and the blue dotted curve for the stars with a disc size between 20 and 200 au and with a disc mass between 4.2 $M_{\rm Jupiter}$ and 35.6 $M_{\rm Jupiter}$.

been calculated from the spectral energy distribution from centimetre to submillimetre wavelengths and of the interferometric response to the cloud background for 26 out of 55 *HST*-identified proplyds (Mann & Williams 2009). They show that the number of discs per logarithmic mass interval is approximately constant over almost a decade in mass between 4.2 and 35.6 $M_{\rm Jupiter}$. Because these discs were selected to have bright millimetre emission, the sample is biased towards relatively large discs between 20 and 200 au (Mann & Williams 2009). Our rather limited understanding of the initial disc mass, the radial density profile and therefore of the effect of encounters on these discs, limits the validity of comparing the observations with the simulations.

In Fig. 7, we present the cumulative mass distribution of several simulations and compare them with the observed mass distribution. Apart from the Plummer initial conditions, it appears to be difficult to exclude any of the model simulation in Table 1. Our assumption of an initial disc mass of 10 per cent of the zero-age stellar mass is quite arbitrary. If we would have adopted half this value, the curves in Fig. 7 skew somewhat to the left the tree overlapping curves (black, blue dashed and green dash–dotted curves) just staying above the observed distribution, whereas the blue dotted curve ($N = 1500$, $R = 0.5$pc, $Q = 0.1$, $i = 2.0$) compares best with the observations.

In Fig. 8, we compare the mass functions for all stars with those with a selected disc sizes and masses. Stars with a massive disc ($m_{\rm disc} > 4.2$ $M_{\rm Jupiter}$) have considerably higher massed ($\langle m\rangle \simeq 0.34$ M$_\odot$) whereas those with a relatively large disc ($r_{\rm disc} > 100$ au) tend to be somewhat less massive than average ($\langle m\rangle \simeq 0.22$ M$_\odot$).

The majority of simulations with rather cold initial temperature ($Q = 0.1$) fail to reproduce the observed disc distribution. Exceptions are simulations born with a fractal dimension of 1.6, which is also preferred for the disc-size distribution. Most simulations with a virial temperature of $Q = 0.3$ and $Q = 0.5$ provide a satisfactory comparison with the observations.

4 DISCUSSION AND CONCLUSIONS

We have performed simulations of self-gravitating stellar systems in which we incorporated a semi-analytic prescription for the effect of encounters on the sizes and masses of circumstellar discs. Our simulations aim at reproducing the disc-size distribution observed around 95 stars in the Trapezium cluster (Vicente & Alves 2005) and with the 23 observed disc masses (Mann & Williams 2009).

Our simulations ignore most physical effects that tend to play an important role in the evolution of these systems, these include the presence of residual gas from the parent molecular cloud, the tidal field of the Galaxy, primordial binaries and mass segregation, stellar evolution, and feedback process. The only aspect we take into account properly in our simulations are the gravitational encounters between stars. We estimate, at run time, how circumstellar discs are truncated as a result of two-body encounters. Regardless of the limited physics in our simulations the resulting disc-size distribution compares excellently with the observations. The disc-mass distribution gives a consistent picture, but is less constraining due to the smaller number of observed masses. Bolstered by our success to reproduce the observed disc radius distribution from the simple argument that this distribution originates from close encounters in the young star clusters, we use this argument to limit some of the structure parameters of the cluster at an earlier age.

The disc-size distribution appears to match the observations best if the Trapezium cluster was born virialized ($Q = 0.5$) or slightly colder ($Q = 0.3$) and with a half-mass (or characteristic) radius of $R \simeq 0.5$ pc. Due to the large run-to-run variations it is hard to constrain these values further. With these parameters the best comparison is achieved for clusters with $N = 2500$–3000 stars.

Simulations with a smaller number of stars tend to underproduce the number of stars in the range where discs have been observed, whereas in more massive cluster discs tend to be harassed on too short a time-scale.

We exclude a Plummer sphere as the initial density profile, irrespective of the initial cluster radius, because too few discs are truncated. Even with cold initial conditions $Q = 0.1$ and a tiny radius $R = 0.125$, the Plummer sphere will always have some stars that remain insufficiently affected by dynamical encounters within

the available time. For similar reasons, we also exclude the density distribution with a relatively high fractal dimension $F \gtrsim 2$, and cluster with a large characteristic radius of $R \gtrsim 0.7$ pc, irrespective of the kinematic temperature of the initial cluster. Clusters with a fractal initial distribution of stars, with relatively cold initial conditions or a small characteristic radius $R \lesssim 0.3$ pc are also excluded, because they truncate too many discs too effectively.

An initial density distribution generated using a fractal dimension of $F = 1.6$ result in the best comparison with the observations, although the number of stars should then be between $N = 2500$ and 3000, the virial temperature of $Q \simeq 0.3$–0.5, and with a half-mass radius of $R \simeq 0.5$ pc.

These results are robust against small changes in the initial conditions. Additional simulations with a Salpeter mass function with a lower mass limit of 0.1 $M_\odot$, have no appreciable effect on the results. Our prescription for the mass evolution in close encounter depends on the initially adopted disc size, for which we adopted 400 au. We performed additional simulations with initial disc radii of 1000 au, but this had no appreciable effect on the resulting disc-mass size distribution.

We have not studied the effect of primordially mass segregation, but we think that the effect somewhat mimics a slight reduction in the initial kinematic temperature. It could therefore be preferable to start with slightly warmer initial distributions if the degree of initial mass segregation is appreciable.

The distributions of disc sizes and masses for stars that have escaped the cluster are not appreciably different than those that remain bound, irrespective of the age of the cluster. Stars tend to escape after a strong encounter and the discs have already been truncated by that time.

4.1 Further considerations

The Solar system may have been truncated at about 35 au by a close encounter with another star (Jílková et al. 2015). According to our calculations a truncation between 10 and 100 au occurs in about 25 per cent of the planetary systems born in a cluster with parameters similar to the Trapezium cluster. The parameters of the Trapezium clusters, as constrained by our calculations, are not inconsistent with the possible parameters of the cluster in which the Sun was born (Portegies Zwart 2009), although there the anticipated cluster was slightly larger, 2 ± 1 pc and probably somewhat more massive (2000 ± 1000 $M_\odot$). We still favour this larger cluster radius for forming the Solar system, because of the need to also survive the ablation of the protoplanetary disc by the ablation of supernovae. This process happens at a somewhat later time ($\gtrsim$5 Myr), and is not accounted for in our simulations.

With the parameters that give a best comparison with the Trapezium cluster, ∼70 per cent of discs are truncated below ∼10 au within the first few hundred thousand years of their dynamical evolution. Further truncation may be initiated by photoevaporation of the massive stars in the young cluster (Adams et al. 2004), but that does not effect the earlier evolution studied here. Violent disc truncation may not particularly hinder the planet formation process, but it sure excludes the formation of planets in orbits beyond the disc truncation radius. Another aspect of the truncation of protoplanetary discs may be the exclusion of Earth-like ice giants, which are expected to form well beyond the ice line ($a \gtrsim 10$ au), and subsequently sink closer to the star in the remaining disc via what is called the grand tack model (Morbidelli, Gaspar & Nesvorny 2014; Deienno et al. 2015)

In a recent study, Vincke et al. (2015) conclude that mutual stellar encounters are responsible for truncating protoplanetary discs in young small clusters; in clusters with an average density of 60 star pc^{-3}, such as the Orion nebula cluster, up to 65 per cent of protoplanetary discs are truncated below 1000 au, whereas 15 per cent is truncated even below 100 au. In a more dense environment (500 star pc^{-3}), these fractions increase to 85 per cent and 39 per cent. Our calculations are consistent with the analysis of Vincke et al. (2015), but in order to reproduce the disc-size distribution observed in the Orion Trapezium cluster the initial cluster density has to be much higher, $\sim 10^3$ star pc^{-3}.

It is interesting to note that all stars in the simulations that reproduced the disc-size distribution observed in the Orion Trapezium cluster have captured some material from the discs of other stars. In our most favourite simulation for the Trapezium cluster ($N = 2000$, $R = 0.5$ pc, $Q = 0.5$, $F = 1.6$), about 60 per cent of the stars have captured $\gtrsim$1 per cent of their own disc mass from another star in a close encounter, and ∼34 per cent captured more than 10 per cent of mass. This is consistent with the idea proposed by Jílková et al. (2015) for the origin of the planetesimal Sedna, being captured from another star in the early evolution of the Solar system.

ACKNOWLEDGEMENTS

We thank Anthony Brown, Michiel Hogerheijde, Lucie Jílková and Igas Snellen for discussions. This work was supported by the Netherlands Research Council NWO (grants #643.200.503, #639.073.803 and #614.061.608) by the Netherlands Research School for Astronomy (NOVA). The numerical computations were carried out on the Little Green Machine at Leiden University.

REFERENCES

Adams F. C., Hollenbach D., Laughlin G., Gorti U., 2004, ApJ, 611, 360
Andrews S. M., Wilner D. J., Hughes A. M., Qi C., Dullemond C. P., 2009, ApJ, 700, 1502
Andrews S. M., Wilner D. J., Hughes A. M., Qi C., Dullemond C. P., 2010, ApJ, 723, 1241
Breslau A., Steinhausen M., Vincke K., Pfalzner S., 2014, A&A, 565, A130
de Juan Ovelar M., Kruijssen J. M. D., Bressert E., Testi L., Bastian N., Cánovas H., 2012, A&A, 546, L1
de Zeeuw P. T., Hoogerwerf R., de Bruijne J. H. J., Brown A. G. A., Blaauw A., 1999, AJ, 117, 354
Deienno R., Gomes R. S., Morbidelli A., Walsh K. J., Nesvorny D., 2015, AAS/Division of Dynamical Astronomy Meeting, Vol. 46, #300.04
Goodwin S. P., Whitworth A. P., 2004, A&A, 413, 929
Hillenbrand L. A., 1997, AJ, 113, 1733
Hillenbrand L. A., Hartmann L. W., 1998, ApJ, 492, 540
Huygens C., 1899, in Bosscha J., Jr, ed., Oeuvres Complètes. Tome VIII. Correspondance 1676-1684. Martinus Nijhoff, Den Haag
Jílková L., Portegies Zwart S., Pijloo T., Hammer M., 2015, MNRAS, 453, 3157
Kolmogorov A. N., 1954, Dokl. Akad. Nauk SSSR, 98, 527
Kroupa P., 2001, MNRAS, 322, 231
López-Sepulcre A., Kama M., Ceccarelli C., Dominik C., Caux E., Fuente A., Alonso-Albi T., 2013, A&A, 549, A114
Mann H., Whitney D., 1947, Ann. Math. Stat., 18, 50 (MW)
Mann R. K., Williams J. P., 2009, ApJ, 694, L36
Morbidelli A., Gaspar H. S., Nesvorny D., 2014, Icarus, 232, 81
Olczak C., Pfalzner S., Spurzem R., 2006, ApJ, 642, 1140
Pelupessy F. I., van Elteren A., de Vries N., McMillan S. L. W., Drost N., Portegies Zwart S. F., 2013, A&A, 557, A84
Plummer H. C., 1911, MNRAS, 71, 460

Portegies Zwart S. F., 2009, ApJ, 696, L13
Portegies Zwart S., Boekholt T., 2014, ApJ, 785, L3
Portegies Zwart S. F., McMillan S. L. W., Hut P., Makino J., 2001, MNRAS, 321, 199
Portegies Zwart S. et al., 2009, New Astron., 14, 369
Portegies Zwart S., McMillan S. L. W., van Elteren E., Pelupessy I., de Vries N., 2013, Comput. Phys. Commun., 183, 456
Prosser C. F., Stauffer J. R., Hartmann L., Soderblom D. R., Jones B. F., Werner M. W., McCaughrean M. J., 1994, ApJ, 421, 517
Reid M. J. et al., 2009, ApJ, 700, 137
Rosotti G. P., Dale J. E., de Juan Ovelar M., Hubber D. A., Kruijssen J. M. D., Ercolano B., Walch S., 2014, MNRAS, 441, 2094
Scally A., Clarke C., 2001, MNRAS, 325, 449
Vicente S. M., Alves J., 2005, A&A, 441, 195
Vincke K., Breslau A., Pfalzner S., 2015, A&A, 577, A115
Wilcoxon F., 1945, Biometrics Bull., 1, 80
Williams J. P., Cieza L. A., 2011, ARA&A, 49, 67

This paper has been typeset from a TEX/LATEX file prepared by the author.